

Evidence for Phonon-Assisted Positronium Emission from Graphite

P. Sferlazzo,⁽¹⁾ S. Berko,⁽¹⁾ K. G. Lynn,⁽²⁾ A. P. Mills, Jr.,⁽³⁾ L. O. Roellig,⁽⁴⁾ A. J. Viescas,⁽⁴⁾
and R. N. West⁽⁵⁾

⁽¹⁾*Brandeis University, Waltham, Massachusetts 02154*

⁽²⁾*Brookhaven National Laboratory, Upton, New York 11973*

⁽³⁾*AT&T Bell Laboratories, Murray Hill, New Jersey 07974*

⁽⁴⁾*City College of the City University of New York, New York, New York 10031*

⁽⁵⁾*University of East Anglia, Norwich NR47TJ, England*

(Received 23 September 1987)

We observe positronium (Ps) emission from a graphite surface being bombarded by slow positrons. The band structure of graphite does not support the usual one-electron-hole process for Ps formation because of conservation of momentum parallel to the surface. A large temperature coefficient for the emission of energetic Ps suggests a new mechanism in which momentum conservation is satisfied by the emission and absorption of phonons. A simple theory including one-phonon processes explains the temperature dependence as well as the angular distribution of the Ps.

PACS numbers: 71.20.Cf, 36.10.Dr, 71.60.+z

Positronium (Ps) emission from metals appears to occur primarily via the sudden capture of an electron near the surface by a thermalized positron.¹ The metal is left in a one-hole excited state and the Ps momentum distribution reflects reasonably well the electronic density of states at and below the Fermi surface.² Shakeup events involving more electron-hole pairs or phonons may be involved with lower probability, and are perhaps responsible for the observed deviation of the Ps angular distribution at low momenta from the predictions of the simplest direct capture model.^{1,3} In graphite, the shape of the electronic bands⁴ is such that this simple Ps emission channel, although energetically allowed, is forbidden by conservation of momentum parallel to the surface. In this Letter we report that graphite does in fact emit Ps, implying the operation of a new higher-order process; a strong temperature dependence of the Ps yield suggests a phonon-assisted emission mechanism. A lowest-order theory incorporating the absorption or emission of one phonon describes well the measured momentum density of the emitted Ps as well as its temperature dependence.

Slow positrons were obtained from self-moderating ⁶⁴Cu sources and were magnetically guided to an ultra-high-vacuum (UHV) target chamber.² The Ps momentum densities were obtained by the two-dimensional angular correlation of annihilation radiation (2D ACAR) technique.⁵ The 2D-ACAR spectra were measured with two Anger cameras, each placed 11 m from the sample. The angular resolution of the apparatus was 1 mrad full width at half maximum, with a typical coincidence rate of 25 sec⁻¹ at the beginning of each run. The ZYA-grade⁶ 12×12×1.5-mm³ highly oriented pyrolytic graphite (HOPG) sample was cleaved in air before mounting. Prior to each several-hour run the sample was heated *in situ* to 1200 K under UHV conditions (10⁻¹⁰ Torr).

Figures 1(a) and 1(b) contain typical room-temperature 2D-ACAR spectra obtained at two incident positron energies: at 12 keV, where ≈93% of the positrons annihilate in the bulk of the sample, and at 750 eV, where they stop close to the surface. In these figures, p_{\perp} and p_{\parallel} are the momenta perpendicular and parallel to the surface; we recall that 2D-ACAR spectra represent one-dimensional integrals (along $\hat{p}_{\parallel} = \hat{p}_{\perp} \times \hat{p}_{\parallel}$) of the 3D momentum density. In HOPG the carbon planes are aligned parallel to the surface (i.e., \hat{p}_{\perp} is along the c axis), with random orientation of the crystallites in the basal plane. The shape of the 12-keV spectrum in Fig. 1(a) is in agreement with recent high-precision bulk 2D-ACAR HOPG experiments.⁷ The 750-eV spectrum in Fig. 1(b) displays the typical asymmetrical Ps emission spectrum^{2,8,9} superimposed on a spectrum that is similar to that of the bulk. Since the Ps is moving away

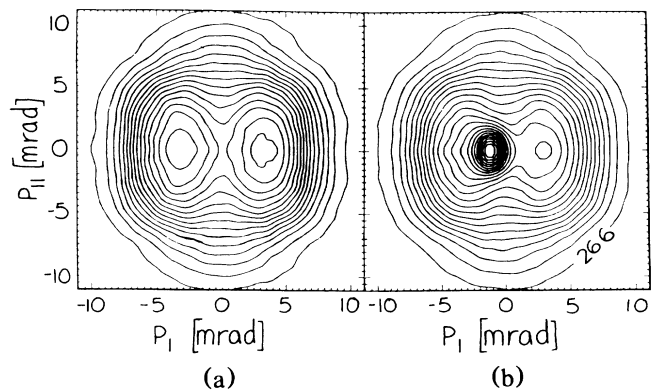


FIG. 1. 2D-ACAR measurements on graphite with (a) 12-keV positrons and (b) 750-eV positrons. To improve the statistics, the spectra have been symmetrized about the $p_{\parallel}=0$ axis. The surface normal is oriented along the $-\hat{p}_{\perp}$ direction.

from the sample surface its momentum density vanishes for $p_{\perp} > 0$, and we can separate the Ps spectrum from the underlying "symmetrical" spectrum.

Before discussing the Ps spectrum, we note a major difference between the HOPG "symmetric" component and the corresponding component in a metal⁸; in metals the symmetric spectrum is due to positron annihilation at the surface (" e^+ surface state"), and its shape is substantially different from the bulk spectrum. In HOPG, the similarity with the bulk indicates that either the positron surface state does not exist and the thermalized positrons annihilate in the last few carbon layers or the electrons sampled by the surface-bound positron are very similar to those sampled by the "interlayer positrons"⁷ in the bulk.

Figure 2(a) shows the Ps emission spectrum obtained at 300 K with 750-eV incident positrons. The theoretical Ps spectrum of Fig. 2(b) will be discussed later. The experimental spectrum is similar to the Ps spectra from Al surfaces, but has a lower maximum Ps momentum: The corresponding Ps energy cutoff is the negative of the Ps work function, $\phi_{Ps} \approx -0.6$ eV. Photoemission¹⁰ and secondary-electron¹¹ measurements yield a 4.7-eV electron work function in graphite. Since $\phi_{Ps} = \phi_+ + \phi_- - 6.8$ eV, we deduce a positron work function $\phi_+ \approx 1.5$ eV, in good agreement with the recent result of Gullikson and Mills.¹²

From the relative intensity of the Ps 2D-ACAR component (only p -Ps contributes), we deduce a total Ps yield (p -Ps plus o -Ps) of about 16% at 300 K for a 200-eV positron incident energy. We have obtained similar 2D-ACAR spectra at 120, 850, and 1250 K; the total Ps yield is found to increase nearly linearly with tempera-

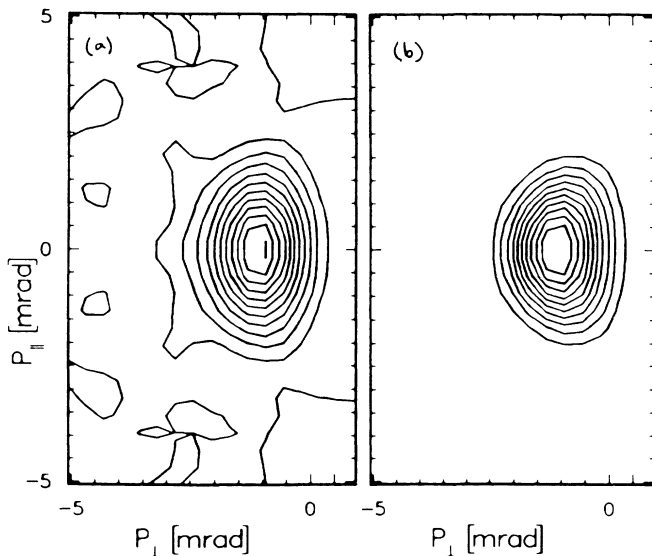


FIG. 2. 2D projections of the Ps emission momentum spectra from graphite: (a) experiment and (b) phonon-assisted Ps emission theory.

ture to $\approx 50\%$ at 1250 K. On the other hand, the shape of the Ps spectra changes only slightly as a result of thermal broadening. This temperature behavior is again very different from that observed in Al and other metals. There a thermal-energy Ps peak grows with temperature because of the desorption of the positron surface state. When the shape of the remaining symmetrical spectrum is analyzed at 850 and 1250 K, we find that the "bulk"-like shape decreases as the Ps yield increases, revealing a narrow conical distribution of (5–10)% intensity. A possible explanation is that we are seeing some positron annihilation in bulk or surface defects. We note that the yield change is probably not associated with the small change in ϕ_{Ps} with temperature.

Since the 2D-ACAR experiments are time consuming, we have studied the full temperature dependence of the Ps yield by measuring the emission fraction¹³ f as a function of energy and temperature using a Ge detector. From these measurements we also obtain $E_0 = 2.4$ keV, the incident positron energy at which f falls to half of its value at the lowest energy. E_0 is related to the thermalized positron diffusion constant. Because E_0 changes by only a few percent over a 50–1200-K temperature range, the increase in f is not likely to be associated with unusual bulk temperature behavior.

The Ps fraction f obtained at 300-eV incident positron energy is shown in Fig. 3 as a function of temperature. We note the linear increase in f above room temperature, and a leveling off below room temperature. The data below room temperature were taken with a different manipulator, and the small mismatch around 300 K might be due to this change. The falloff in f at the lowest T is probably due to the accumulation of condensed residual gases. The data of Fig. 3 are not inconsistent with the temperature-dependent Ps formation probability found in Grafoil and powdered graphite^{14,15}; the very small Ps intensity (0.3%) observed in bulk HOPG by 2D ACAR⁷ might also be consistent with the present picture if the Ps is formed at inner surfaces.

The large temperature effect leads us to formulate a phonon-assisted Ps emission mechanism. The electronic

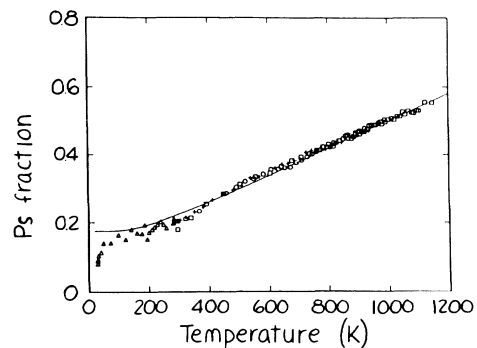


FIG. 3. Positronium fraction vs temperature for slow positrons on graphite.

structure of graphite⁴ reveals filled bands and electron and hole Fermi surfaces of very small cross section along the HKH zone edges. Energy conservation permits all electrons within a region of ≈ 0.6 eV below the Fermi energy to take part in Ps formation and emission. In graphite these electrons correspond to the top of the filled bands situated around the zone edges; the contribution of the few conduction electrons ($\approx 10^{-4}$ electron per atom) is negligible. Parallel momentum conservation, however, rules out these electrons, since they would have to produce Ps of much higher energy than 0.6 eV. Higher-order interactions are needed to provide a mechanism for lowering the k_{\parallel} momenta, such as additional electron-hole pair creation or phonon absorption and emission. However, it is hard to conceive that electron-hole many-body effects could explain the observed large temperature dependence.

We thus explore the simplest phonon mechanism, making the following assumptions: (1) Ps emission takes place close to the surface when a thermalized positron with momentum $k_{+} \approx 0$ interacts with an electron near the zone edge while the high k_{\parallel} is taken up by the emission or absorption of a phonon of appropriate momentum q . Each electron near the zone edge that is energetically allowed to form Ps is thus mapped onto a hemispherical shell of Ps momenta. Such mapping requires phonons with momenta within about one-third of the ΓK distance of the zone edges. (2) For simplicity, we assume that all these phonons have the average energy,¹⁶ $E_{ph} = 440 \text{ cm}^{-1} = k_B \times (630 \text{ K}) \approx 50 \text{ meV}$. (3) We neglect this energy compared to $-\phi_{Ps} \approx 0.6 \text{ eV}$. (4) We also neglect absorption from higher branches so that the sum of the

phonon emission and absorption rates is proportional to

$$\Gamma(T) = a \{2n + 1 + b\}, \quad (1)$$

where $n = \{\exp(E_{ph}/kT) - 1\}^{-1}$ is the phonon occupation number, a is a normalization constant, and b is included to take into account possible effects of spontaneous emission from higher-energy phonon branches.

We evaluate the Fermi "golden rule" for the phonon-assisted Ps emission process making the following additional assumptions: (5) We use a linear E vs k dispersion for the electrons near the zone edge KHK so that the number of electrons available at each Ps energy E_{Ps} is proportional to Δk , the distance between \mathbf{k} and ΓK , the k_{\parallel} component of the crystal momentum of an electron at the zone edge. (6) The Ps emission rate is proportional to the Ps density of final states times the electron density multiplied by $\Gamma(T)$ of Eq. (1). (7) Neglecting the possible \mathbf{k} , \mathbf{k}_{Ps} , \mathbf{q} , and T dependence of the interaction Hamiltonian, we obtain

$$\begin{aligned} dP(\mathbf{k}_{Ps}, T) &= \Gamma(T) d^3 k_{Ps} \Delta k \\ &= \Gamma(T) d\Omega_{Ps} k_{Ps}^2 dk_{Ps} (-\phi_{Ps} - E_{Ps})^{1/2}. \end{aligned} \quad (2)$$

We check the T dependence of dP by fitting Eq. (1) to the Ps fraction data of Fig. 3. A reasonably good fit is obtained with $b < 0.2$, indicating the suppression of the emission of phonons in the higher-energy branches. This would follow from a picture that correlates the phonon emission rate to the presence of the phonon cloud that produces the static deformation around the positron.

In order to test the k_{Ps} dependence of the predicted Ps emission probability dP of Eq. (2), we compare in Fig. 4

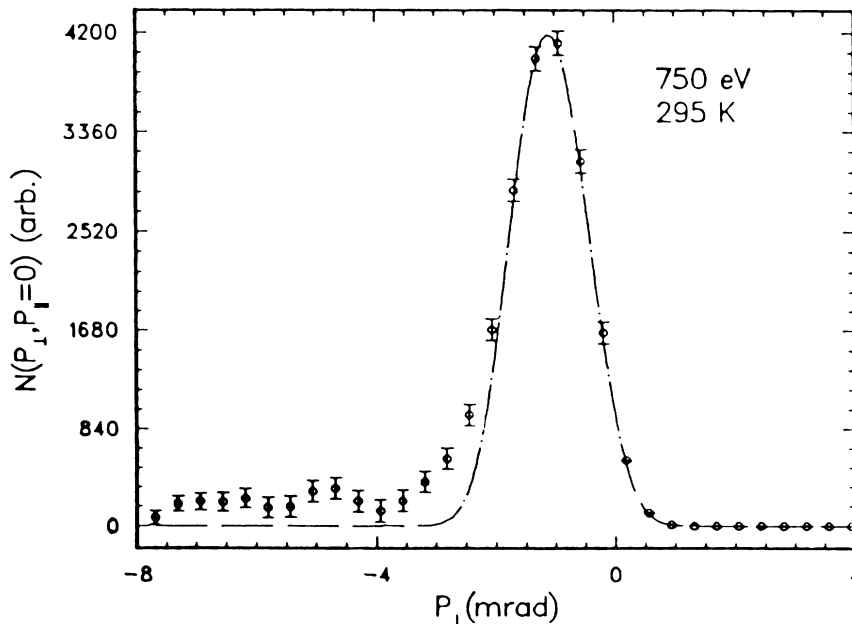


FIG. 4. A $p_{\parallel} = 0$ cut through the 2D-ACAR positronium spectrum of Fig. 2 and the theoretical curve obtained with use of Eq. (2).

a cut through the observed 2D-ACAR Ps spectrum with the corresponding cut through dP after convolution of Eq. (2) with the 2D resolution of the apparatus. The best fit obtained yields $\phi_{Ps} = -0.55 \pm 0.05$ eV. The fit is good except at the highest Ps energies where we observe some Ps attributable to nonthermalized positrons. The complete 2D Ps spectrum corresponding to this fit is shown as a contour map in Fig. 2(b), indicating a good overall agreement with the 2D data. We note that the analogous process replacing the phonon with an electron-hole pair gives an identical momentum density, but with no temperature dependence. The low amplitude of the electron-hole-assisted emission is reasonable because the requirement of satisfying the free Ps momentum-energy relation excludes direct electron-hole pairs and restricts the available phase space for indirect processes.

In summary, evidence for a new Ps emission mechanism has been obtained by the study of the momentum distribution and temperature dependence of the Ps emitted from oriented graphite samples. A simple theory for phonon-assisted Ps formation gives good agreement with our observation. In metals such as Al, where direct capture is not forbidden as it is in graphite, a similar phonon-assisted mechanism should also operate, but at a much reduced level; such effects also seem to play a role in angle-resolved photoemission.¹⁷ The agreement of our observations with simple theory gives further credence to our interpretation of the angle-resolved Ps emission spectra of simple metals^{1,2} and makes it likely that the method can be extended to other interesting systems.

The authors would like to thank P. M. Platzman, K. F. Canter, D. M. Chen, and J. Zahradka for valuable assistance. This work was supported in part by the National Science Foundation through Grant No. DMR-8315691 and the U. S. Department of Energy Division of Materials Sciences under Contract No. DE-AC02-

76CH00016.

¹A. P. Mills, Jr., L. Pfeiffer, and P. M. Platzman, *Phys. Rev. Lett.* **51**, 1085 (1983).

²D. M. Chen, S. Berko, K. F. Canter, K. G. Lynn, A. P. Mills, Jr., L. O. Roellig, P. Sferlazzo, M. Weinert, and R. N. West, *Phys. Rev. Lett.* **58**, 921 (1987).

³J. B. Pendry, private communication cited in R. Howell, P. Meyer, I. J. Rosenberg, and M. J. Fluss, *Phys. Rev. Lett.* **54**, 1698 (1985).

⁴See, for example, R. C. Tatar and S. Rabii, *Phys. Rev. B* **25**, 4126 (1982), and references therein.

⁵S. Berko, in *Positron Solid State Physics*, edited by W. Brandt and A. Dupasquier (North-Holland, Amsterdam, 1983), p. 64.

⁶Manufactured by Union Carbide Corp., Carbon Products Division, Cleveland, OH 44101.

⁷R. R. Lee, E. C. von Stetten, M. Hasegawa, and S. Berko, *Phys. Rev. Lett.* **58**, 2363 (1987).

⁸K. G. Lynn, A. P. Mills, Jr., R. N. West, S. Berko, K. F. Canter, and L. O. Roellig, *Phys. Rev. Lett.* **54**, 1702 (1985).

⁹Howell *et al.*, Ref. 3.

¹⁰See, for example, A. R. Law, J. J. Barry, and H. P. Hughes, *Phys. Rev. B* **28**, 5332 (1983).

¹¹R. G. Willis, B. Fitton, and G. J. Painter, *Phys. Rev. B* **9**, 1926 (1974).

¹²E. M. Gullikson and A. P. Mills, Jr., *Phys. Rev. B* **36**, 8777 (1987).

¹³A. P. Mills, Jr., in Ref. 5, p. 432.

¹⁴Y. C. Jean, *Appl. Phys. A* **35**, 169 (1984).

¹⁵P. Rice-Evans, M. Moussavi-Madani, K. U. Rao, D. T. Britton, and B. P. Cowan, *Phys. Rev. B* **34**, 6117 (1986).

¹⁶See, for example, R. Al-Jishi and G. Dresselhaus, *Phys. Rev. B* **26**, 4514 (1982), and references therein.

¹⁷N. J. Shevchik, *Phys. Rev. B* **16**, 3428 (1977); Z. Hussain, E. Umbach, J. J. Barton, J. G. Tobin, and D. A. Shirley, *Phys. Rev. B* **25**, 672 (1982).